

## Supplementary Information

# **A highly luminescent 3-phenylfluoranthene-modified g-C<sub>3</sub>N<sub>4</sub> derivative used as a metal-free phosphor in white light-emitting diodes**

Jinghao Zhang,<sup>1</sup> Long Wang,<sup>1</sup> Huaijun Tang,\* Xiang Li, Aijing Jiang, Yibing Wu,\* Shanglan Xian, Rongman Xia, Yifei Li, Zhouyang Jiang and Zhengliang Wang

*Key Laboratory of Green-Chemistry Materials in University of Yunnan Province, National and Local Joint Engineering Research Center for Green Preparation Technology of Biobased Materials, School of Chemistry & Environment, Yunnan Minzu University, Kunming 650500, P. R. China.*

\*Corresponding Author: Prof. Huaijun Tang

E-mail: tanghuaijun@sohu.com

\*Corresponding Author: Dr. Yibing Wu

yibingwu@ymu.edu.cn

<sup>1</sup>These authors contributed equally to this work.

## 1. General information

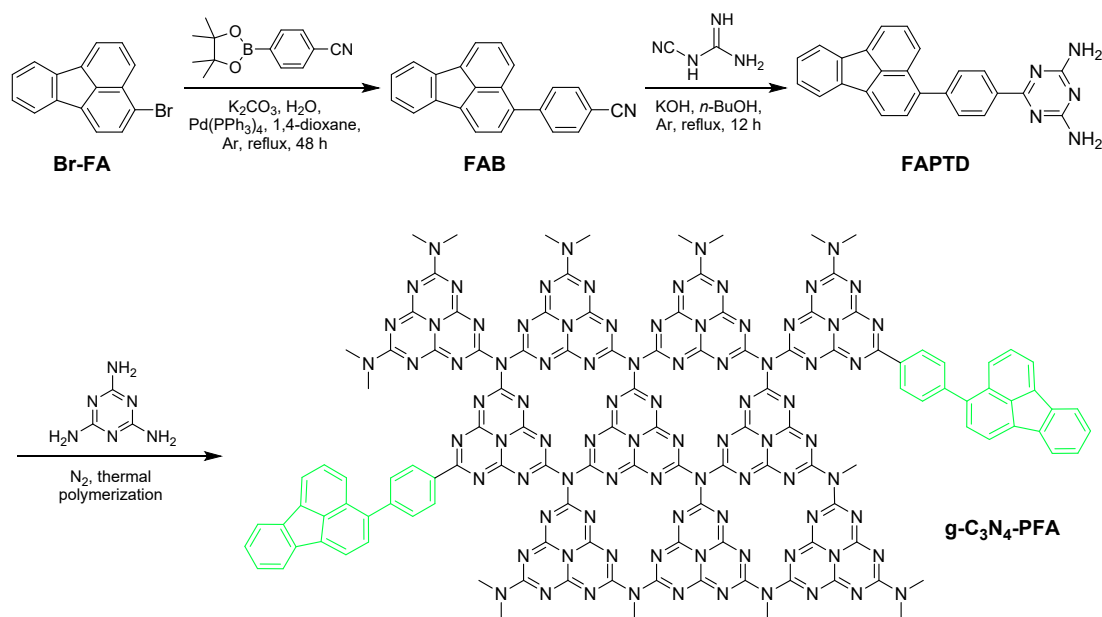
All chemicals and reagents for organic synthesis were purchased from Shanghai Titan Scientific Co. Ltd. (in Shanghai, China) and used without further purification.  $\text{K}_2\text{SiF}_6\cdot\text{Mn}^{4+}$ , epoxy resin and GaN-based blue-light chips ( $\lambda_{\text{em,max}} \approx 460$  nm,  $\text{LE} \approx 25$   $\text{lm}\cdot\text{W}^{-1}$ ) were purchased from Shenzhen Zhanwanglong Technology Co. Ltd (in Shenzhen, China).

$^1\text{H}$  NMR and  $^{13}\text{C}$  Solid-state NMR ( $^{13}\text{C}$  SSNMR) spectra were obtained by a Bruker AVANCE III 400 M spectrometer (Bruker, Germany). Fourier transform infrared (FTIR) spectra were obtained via KBr pellets containing samples by a Nicolet iS10 FT-IR spectrometer (ThermoFisher Scientific, U.S.A.). Powder X-ray diffraction (PXRD) patterns were recorded on a Bruker AXS D8 Advance A25 Powder X-ray Diffractometer (Bruker, Switzerland) using graphite monochromatized  $\text{Cu K}\alpha$  radiation ( $\lambda = 1.5406$  Å, 40 kV and 40 mA). The morphology of samples was observed by a FEI Nova NanoSEM450 scanning electron microscopy (SEM, FEI Company, U.S.A.). Thermogravimetry (TG) and derivative thermogravimetry (DTG) curves were obtained by a Netzsch STA449F3 thermal analyzer ( $10$  °C $\cdot\text{min}^{-1}$ , under  $\text{N}_2$ ). Photoluminescence (PL) spectra at ambient temperature and the temperature dependent PL spectra were measured on a Hitachi F-7000 PL spectrophotometer (Hitachi Co., Ltd, Japan), the temperature was controlled by a REX-C110 temperature controller (Kaituo Compressor Parts Co., Ltd, China). PL decay curve and PL quantum yield of g- $\text{C}_3\text{N}_4$ -PFA were measured by an Edinburgh FS5 spectrofluorometer (Edinburgh Instruments Ltd., UK). The ultraviolet-visible-near infrared diffuse reflectance spectra (UV-Vis-NIR DRS) were measured by a Hitachi U-4100 spectrophotometer (Hitachi Co., Ltd, Japan). Electron density distribution and energy values of the LUMOs and HOMOs of g- $\text{C}_3\text{N}_4$  and g- $\text{C}_3\text{N}_4$ -PFA models were calculated by density functional theory (DFT) in the Gaussian16 suite of programs.

## 2. Synthesis of 4-(fluoranthen-3-yl)benzotrile (FAB)

The preparation route to g- $\text{C}_3\text{N}_4$ -PFA is shown in Scheme S1 (also as Scheme 1

shown in text of the Communication), the details of the preparation process are described as follows.



**Scheme S1.** Preparation route to  $g\text{-C}_3\text{N}_4\text{-PFA}$ .

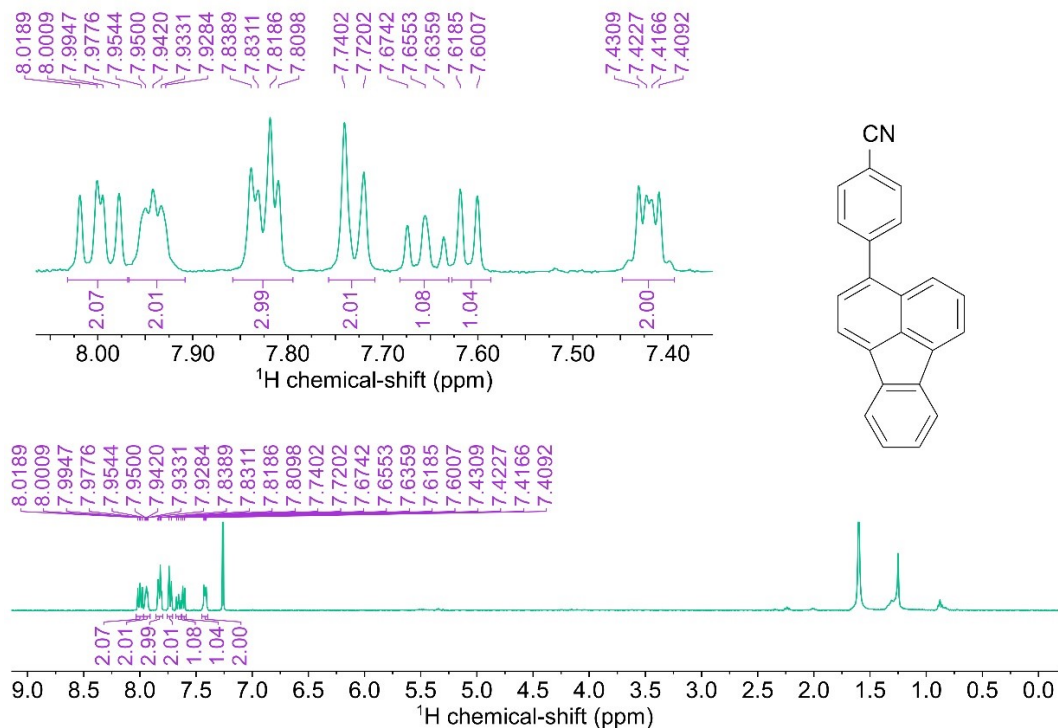


**Fig. S1.**  $^1\text{H}$  NMR spectrum of 4-(fluoranthren-3-yl)benzonitrile (FAB)

Anhydrous  $\text{K}_2\text{CO}_3$  (8.7 g, 63.0 mmol) was added in water (12.0 mL), then 3-bromofluoranthene (Br-FA, 5.0 g, 17.8 mmol), 4-(4,4,5,5-tetramethyl-1,3,2-

dioxaborolan-2-yl)benzotrile (8.2 g, 35.8 mmol) and 1,4-dioxane (60.0 mL) were added in the mixture. After purging the mixture with Ar to remove O<sub>2</sub> by bubbling, Pd(PPh<sub>3</sub>)<sub>4</sub> (1.0 g, 0.87 mmol) was added. The mixture was refluxed with stirring under Ar for 48 h. After being cooled to room temperature, water (100.0 mL) was added into the reaction mixture. Then, the mixture was extracted with CH<sub>2</sub>Cl<sub>2</sub> (3 × 100 mL), the organic phase was washed with saturated brine (3 × 25 mL) and dried by anhydrous MgSO<sub>4</sub>. The solvent was removed by vacuum rotary evaporation, the residues were chromatographed on a silica gel column eluting with a mixed solvent of petroleum ether (60~90 °C) and CH<sub>2</sub>Cl<sub>2</sub> (volume rate, 2:1), the obtained solid was further purified by recrystallization using petroleum ether (60~90 °C) and CH<sub>2</sub>Cl<sub>2</sub> (volume rate, 2:1), the product was obtained as pale yellow-green needles, yield was 85.3% (4.6 g). <sup>1</sup>H NMR (400 MHz, CDCl<sub>3</sub>, ppm, Fig. S1): δ = 8.00 (d, <sup>3</sup>J = 7.2 Hz, 1H, ArH), 7.99 (d, <sup>3</sup>J = 6.8 Hz, 1H, ArH), 7.94 (t, <sup>3</sup>J = 3.6 Hz, 2H, ArH), 7.80–7.85 (m, 3 H, ArH), 7.73 (d, <sup>3</sup>J = 8.0 Hz, 2H, ArH), 7.66 (d, <sup>3</sup>J = 7.6 Hz, 1H, ArH), 7.40–7.44 (m, 2 H, ArH).

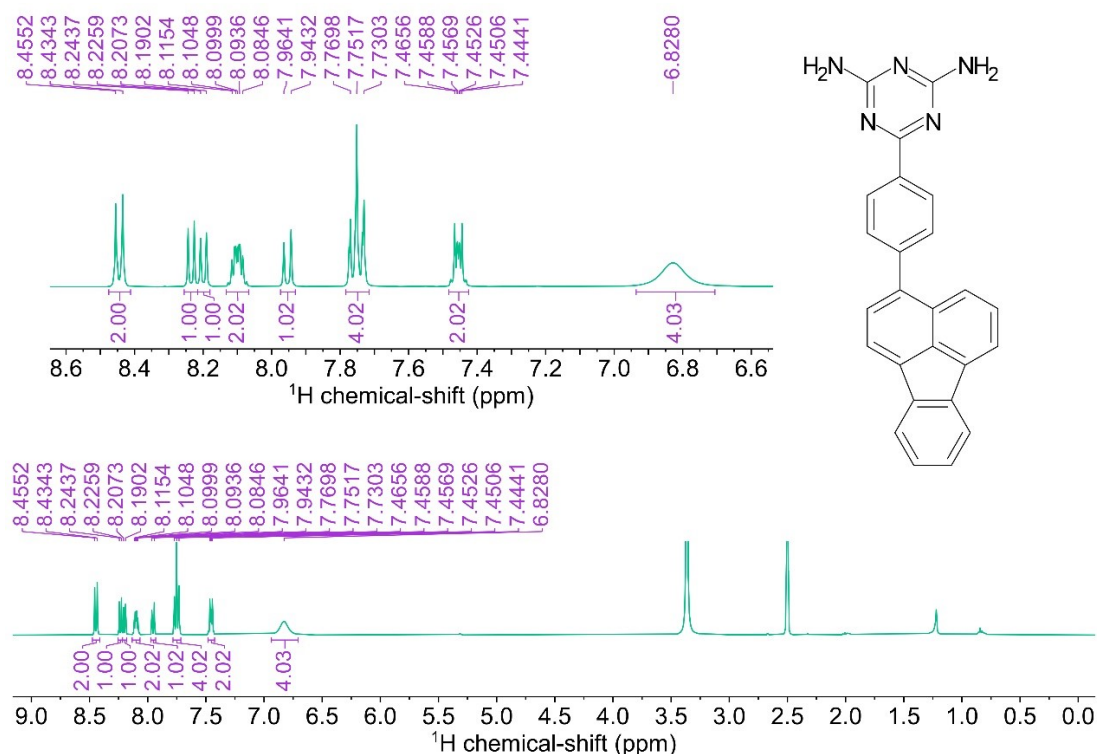


**Fig. S2.** <sup>1</sup>H NMR spectrum of 6-(4-(fluoranthren-3-yl)phenyl)-1,3,5-triazine-2,4-diamine (FAPTD)

### 3. Synthesis of 6-(4-(fluoranthren-3-yl)phenyl)-1,3,5-triazine-2,4-diamine (FAPTD)

The previously obtained FAB (4.6 g, 15.2 mmol), dicyandiamide (2.2 g, 25.8 mmol) and KOH (1.2 g, 21.4 mmol) were added in *n*-butanol (150.0 mL), then the mixture was refluxed with stirring under Ar for 12 h. After being cooled to room temperature, the resulting precipitate was filtered, washed successively with hot water (60 °C, 4 × 500 mL), CH<sub>3</sub>OH (3 × 100 mL) and CH<sub>2</sub>Cl<sub>2</sub> (3 × 100 mL). The product was obtained as yellow-green powders, yield was 83.4% (4.9 g). <sup>1</sup>H NMR (400 MHz, DMSO-D<sub>6</sub>, ppm, Fig. S2): δ = 8.44 (d, <sup>3</sup>J = 8.4 Hz, 2H, ArH), 8.23 (d, <sup>3</sup>J = 7.2 Hz, 1H, ArH), 8.20 (d, <sup>3</sup>J = 6.8 Hz, 1H, ArH), 8.08–8.12 (m, 2H, ArH), 7.95 (d, <sup>3</sup>J = 8.4 Hz, 1H, ArH), 7.72–7.78 (m, 4H, ArH), 7.42–7.48 (m, 2H, ArH), 6.83 (s, 4H, -NH<sub>2</sub>).

### 4. Preparation of g-C<sub>3</sub>N<sub>4</sub>-PFA and g-C<sub>3</sub>N<sub>4</sub>

A series of g-C<sub>3</sub>N<sub>4</sub>-PFA were prepared via under different molar ratios of melamine and FAPTD, different calcination temperatures and durations, and the specific details are described as follows. Melamine and FAPTD (molar ratios, 5:1, 10:1, 15:1, 20:1 or 25:1) were added in an agate mortar and ground thoroughly to ensure uniform mixing (for ca. 0.5 h). The resulting fine powders were put into a corundum crucible (with a diameter of 18 mm and a height of 26 mm), then the crucible was wrapped by a piece of aluminium foil. After two vent holes in aluminium foil on the top of crucible were made by a syringe needle (diameter of 0.45 mm), the crucible was heated (2.5 °C·min<sup>-1</sup>) in N<sub>2</sub> atmosphere to a certain preset temperature (350 °C, 400 °C, 450 °C, 500 °C or 550 °C) and then kept for some time (1.0 h, 1.5 h, 2.0 h, 2.5 h or 3.0 h). After being cooled to room temperature, the products were dug out as yellow solid. The g-C<sub>3</sub>N<sub>4</sub> was synthesized via thermal polymerization (at 500 °C) by using only melamine as precursors.

All samples of g-C<sub>3</sub>N<sub>4</sub>-PFA and g-C<sub>3</sub>N<sub>4</sub> cannot be purified by common purification methods such as purifying by a chromatography column or recrystallization, even the vacuum sublimation method [S1], so they were all directly used in the state as they were prepared.

## 5. Optimization of g-C<sub>3</sub>N<sub>4</sub>-PFA preparation conditions

### 5.1 The optimal molar ratio of melamine and FAPTD

As shown in **Fig. S3**, when molar ratios of melamine and FAPTD changed from 25:1 to 5:1, the doping amount of FAPTD gradually increased, the PL emission spectra showed gradual red shifts, the maximum emission wavelengths ( $\lambda_{em,max}$ ) were 529 nm, 534 nm, 550 nm, 551 nm and 553 nm, respectively. The emission intensity first increased and then decreased, and the maximum value occurred when the ratio was 15:1, which suggested 3-phenylfluoranthene (PFA) can effectively improve the emission intensity (or efficiency) and make the emission red shift, especially relative to those of g-C<sub>3</sub>N<sub>4</sub> [S1]. However, when excessive PFA groups being grafted on heptazines, probably due to local distortion and vibration-rotation correspondingly increasing, energy loss raised and then the emission intensity decreased [S2].

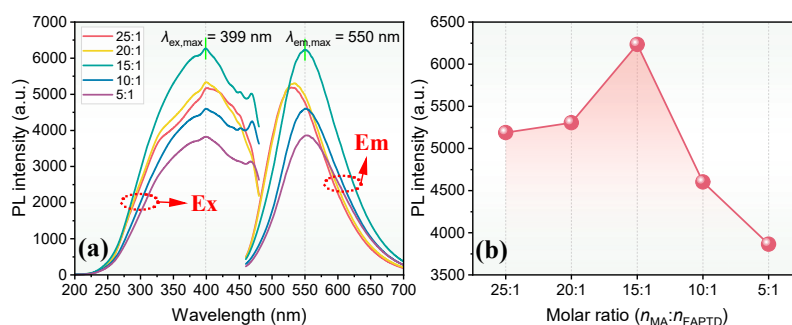


**Fig. S3.** (a) PL excitation (Ex) and emission (Em) spectra of g-C<sub>3</sub>N<sub>4</sub>-PFA samples synthesized using melamine (MA) and FAPTD at different molar ratios (25:1, 20:1, 15:1, 10:1 or 5:1), but all at 450 °C and for 2.0 h. (b) The maximum PL emission intensities of the spectra in figure (a).

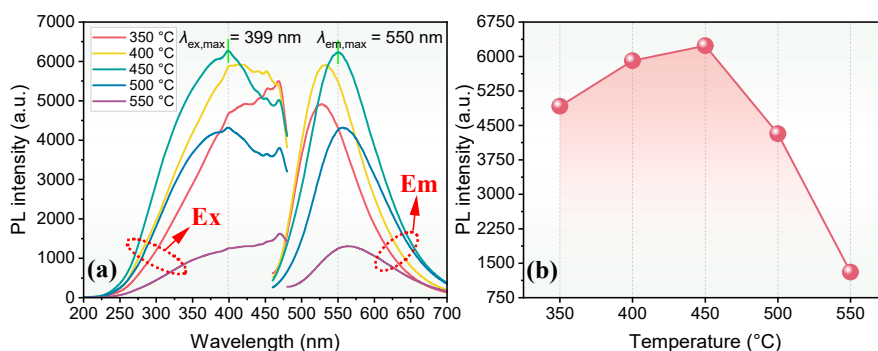


**Fig. S4.** (a) PL excitation (Ex) and emission (Em) spectra of g-C<sub>3</sub>N<sub>4</sub>-PFA samples synthesized at different temperatures (350 °C, 400 °C, 450 °C, 500 °C or 550 °C), but all using melamine and FAPTD at molar ratio of 15:1 and being heated for 2.0 h. (b)

The maximum PL emission intensities of the spectra in figure (a).

## 5.2 The optimal temperature

As shown in **Fig. S4**, from 350 °C to 550 °C, the PL emission spectra also showed gradual red shifts, the  $\lambda_{em,max}$  were 528 nm, 534 nm, 550 nm, 556 nm and 563 nm, respectively. Increasing the temperature was beneficial for the formation of g-C<sub>3</sub>N<sub>4</sub>-PFA 2D sheets. However, if the temperature was too high, the number of defects would increase [S3], resulting in a decrease in emission intensity. The results showed 450 °C was the optimal temperature.

## 5.3 The optimal heating time

As shown in **Fig. S5**, the spectra and their  $\lambda_{em,max}$  were not significantly affected by the heating time. From 1.0 h to 3.0 h, the range of the spectra hardly changed with the increasing time, the  $\lambda_{em,max}$  were 543 nm, 547 nm, 550 nm, 550 nm and 551 nm, respectively. Prolonging the heating time was beneficial for the formation of g-C<sub>3</sub>N<sub>4</sub>-PFA 2D sheets, however, if the heating time was too long, it may increase the number of defects and the degree of aggregation [S3], also resulting in a decrease in emission intensity. The results showed 2 h was the optimal heating time.

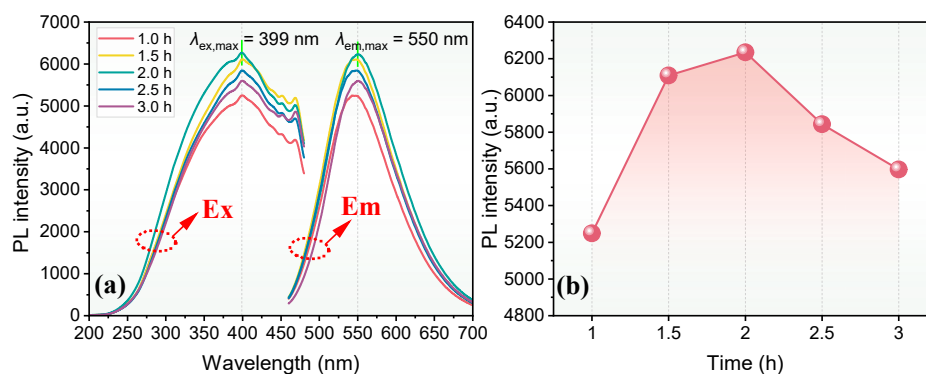


**Fig. S5.** (a) PL excitation (Ex) and emission (Em) spectra of g-C<sub>3</sub>N<sub>4</sub>-PFA samples synthesized at different heating times (1 h, 1.5 h, 2 h, 2.5 h or 3h), but all using melamine and FAPTD at molar ratio of 15:1 and being heated at 450 °C. (b) The maximum PL emission intensities of the spectra in figure (a).

## References

[S1] H. Tang, Q. Chen, G. Meng, S. Lu, et al, *RSC Adv.*, 2023, 13, 12509.

[S2] H. Tang, Q. Chen, S. Lu, et al, *J. Lumin.*, 2022, 244, 118734.

[S3] Y. Wang, F. Dai, Y. Tao, et al, *Inorg. Chem. Front.*, 2024, **11**, 2346–2354.

## 6. Fabrication and performance measurements of LEDs

Phosphors (g-C<sub>3</sub>N<sub>4</sub>-PFA, or g-C<sub>3</sub>N<sub>4</sub>-PFA together with K<sub>2</sub>SiF<sub>6</sub>:Mn<sup>4+</sup>) were added into epoxy resin at different weight percentages (wt.%). After the mixtures being stirred uniformly, they were coated on the GaN-based blue-light chips ( $\lambda_{\text{em,max}} \approx 460$  nm, LE  $\approx 25$  lm·W<sup>-1</sup>) until its reflective cavities just were completely filled. The LEDs were heated to solidify at 50 °C for 2 h. All the LEDs devices were tested under 3.0 V and 20 mA. The emission spectra of the LEDs devices were measured by on a high accurate array spectrometer (HSP6000, HongPu Optoelectronics Technology Co. Ltd, in Hangzhou, China), and their performance data were obtained by a spectroradiometer system with an integrating sphere (PMS-50, Everfine Optoelectronics Technology Co. Ltd, in Hangzhou, China).

## 7. The ultraviolet-visible-near infrared diffuse reflectance spectra (UV-Vis-NIR DRS) and corresponding Tauc plots

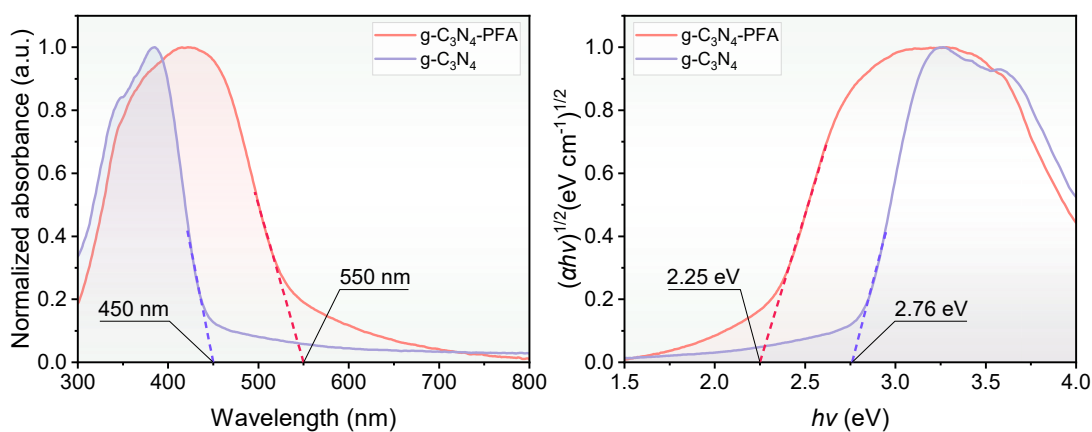


**Fig. S6.** UV–Vis–NIR DRS (a) and corresponding Tauc plots (b) of g-C<sub>3</sub>N<sub>4</sub> and g-C<sub>3</sub>N<sub>4</sub>-PFA.

## 8. Measurement of PL quantum yield (PLQY) of g-C<sub>3</sub>N<sub>4</sub> and g-C<sub>3</sub>N<sub>4</sub>-PFA

In the measurement of PLQY of g-C<sub>3</sub>N<sub>4</sub> and g-C<sub>3</sub>N<sub>4</sub>-PFA, a non-luminescent polytetrafluoroethylene sheet was used as the blank for measuring the baseline. The PLQY was calculated according to the following formula.

$$PLQY = \frac{S_{em,A} - S_{em,B}}{S_{ex,B} - S_{ex,A}}$$

where  $S_{em,A}$  and  $S_{em,B}$  represent the integrated areas of the PL emission (as em) peaks of g-C<sub>3</sub>N<sub>4</sub> or g-C<sub>3</sub>N<sub>4</sub>-PFA (as A) and baseline (as B),  $S_{ex,A}$  and  $S_{ex,B}$  represent the integrated areas of the PL excitation (as ex) peaks of g-C<sub>3</sub>N<sub>4</sub> or g-C<sub>3</sub>N<sub>4</sub>-PFA and baseline. The result of PLQY of g-C<sub>3</sub>N<sub>4</sub> 0.044, and that of g-C<sub>3</sub>N<sub>4</sub>-PFA was 0.367.

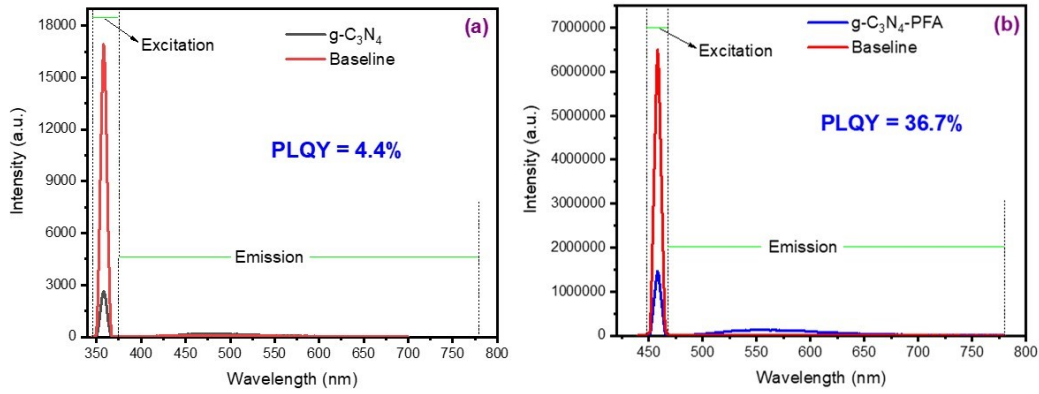


**Fig. S7.** The PL excitation and emission spectra of g-C<sub>3</sub>N<sub>4</sub> and baseline (using non-luminescent polytetrafluoroethylene sheet) (a); g-C<sub>3</sub>N<sub>4</sub>-PFA and baseline (b).

## 9. PL decay curve and its triexponential fitting line of g-C<sub>3</sub>N<sub>4</sub>-PFA powders

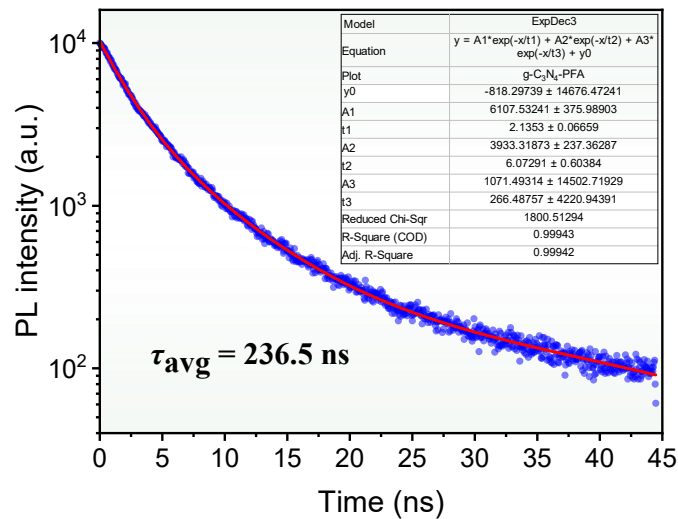


**Fig. S8.** PL decay curve (blue) and its triexponential fitting line (red) of g-C<sub>3</sub>N<sub>4</sub>-PFA powders. Inset: The parameters of triexponential fitting.

**10. Table S1.**  $\lambda_{em,max}$ , the maximum PL emission intensities and corresponding relative intensities ( $\lambda_{ex} = 399$  nm) of g-C<sub>3</sub>N<sub>4</sub>-PFA powders measured at every 20 °C from 30 °C to 210 °C (heating) and from 210 °C to 30 °C (cooling).

Temperature (from 30 °C to 210 °C)	30	50	70	90	110	130	150	170	190	210
$\lambda_{em,max}$ (nm)	554	554	553	552	552	551	551	551	550	550
The maximum intensity (a.u.)	9036	8959	8651	8286	7775	7251	6695	6144	5689	5256
Relative intensity (%)	100.0	99.1	95.7	91.7	86.0	80.2	74.1	68.0	63.0	58.2
Temperature (from 210 °C to 30 °C)	30	50	70	90	110	130	150	170	190	210
$\lambda_{em,max}$ (nm)	553	552	552	551	551	551	551	550	550	550
The maximum intensity (a.u.)	9018	8860	8641	8254	7773	7242	6686	6117	5686	5256
Relative intensity (%)	99.8	98.1	95.6	91.3	86.0	80.1	74.0	67.7	62.9	58.2

**11. Table S2.** Performance data of LEDs No. 1-8.

No. of LEDs	Blending concentrations (wt.%)	LE (lm W <sup>-1</sup> )	CRI	CCT (K)	$\lambda_{em,max}$ (nm)	CIE (x, y)
1	1.00	30.68	40.5	100000	459, 550	(0.19, 0.15)
2	2.00	35.02	76.6	16313	460, 552	(0.26, 0.27)
3	3.00	30.07	73.4	6903	460, 554	(0.30, 0.34)
4	4.00	30.43	66.1	5153	460, 554	(0.35, 0.41)
5	5.00	27.95	61.8	4430	461, 557	(0.38, 0.46)
6	6.00	22.47	60	4256	462, 558	(0.39, 0.48)
7	7.00	22.04	56.2	3714	460, 560	(0.43, 0.50)
8	8.00	20.7	54.1	3404	563	(0.46, 0.51)